The ISME Journal (2013) 7, 1367–1377

www.nature.com/ismej

ORIGINAL ARTICLE

Experimental evolution of nodule intracellular infection in legume symbionts

Su Hua Guan[1,2], Carine Gris[1,2], Stéphane Cruveiller[3], Cécile Pouzet[4,5], Lena Tasse[1,2], Aurélie Leru[4,5], Aline Maillard[1,2], Claudine Médigue[3], Jacques Batut[1,2], Catherine Masson-Boivin[1,2] and Delphine Capela[1,2]

[1]*INRA, Laboratoire des Interactions Plantes-Microorganismes (LIPM), UMR441, Castanet-Tolosan, France;* [2]*CNRS, Laboratoire des Interactions Plantes-Microorganismes (LIPM), UMR2594, Castanet-Tolosan, France;* [3]*CNRS-UMR 8030 and Commissariat à l'Energie Atomique CEA/DSV/IG/Genoscope LABGeM, Evry, France;* [4]*CNRS, Fédération de Recherches Agrobiosciences, Interactions, Biodiversity, Plateforme d'Imagerie TRI, Castanet-Tolosan, France and* [5]*UPS, Fédération de Recherches Agrobiosciences, Interactions, Biodiversity, Plateforme d'Imagerie TRI, Castanet-Tolosan, France*

Soil bacteria known as rhizobia are able to establish an endosymbiosis with legumes that takes place in neoformed nodules in which intracellularly hosted bacteria fix nitrogen. Intracellular accommodation that facilitates nutrient exchange between the two partners and protects bacteria from plant defense reactions has been a major evolutionary step towards mutualism. Yet the forces that drove the selection of the late event of intracellular infection during rhizobium evolution are unknown. To address this question, we took advantage of the previous conversion of the plant pathogen *Ralstonia solanacearum* into a legume-nodulating bacterium that infected nodules only extracellularly. We experimentally evolved this draft rhizobium into intracellular endosymbionts using serial cycles of legume-bacterium cocultures. The three derived lineages rapidly gained intracellular infection capacity, revealing that the legume is a highly selective environment for the evolution of this trait. From genome resequencing, we identified in each lineage a mutation responsible for the extracellular–intracellular transition. All three mutations target virulence regulators, strongly suggesting that several virulence-associated functions interfere with intracellular infection. We provide evidence that the adaptive mutations were selected for their positive effect on nodulation. Moreover, we showed that inactivation of the type three secretion system of *R. solanacearum* that initially allowed the ancestral draft rhizobium to nodulate, was also required to permit intracellular infection, suggesting a similar checkpoint for bacterial invasion at the early nodulation/root infection and late nodule cell entry levels. We discuss our findings with respect to the spread and maintenance of intracellular infection in rhizobial lineages during evolutionary times.
The ISME Journal (2013) **7,** 1367–1377; doi:10.1038/ismej.2013.24; published online 21 February 2013
Subject category: microbe-microbe and microbe-host interactions
Keywords: symbiosis; experimental evolution; rhizobium; infection; genomics

Introduction

Mutualistic symbioses are a major innovation in the living world (Moran, 2006). Mutualism results from coevolution of the two partners leading, ultimately, to cooperation. Intermediate evolutionary stages, however, can be detrimental to one or the other partner and it is unclear which driving forces govern the evolution of mutualism, ensure its maintenance in present systems and its adaptation to environmental challenges (Momeni *et al.*, 2011).

Correspondence: C Masson-Boivin, INRA, Laboratoire des Interactions Plantes-Microorganismes (LIPM), UMR441, CNRS-INRA, CS 52627, F-31326 Castanet-Tolosan, France.
E-mail: catherine.masson@toulouse.inra.fr
Received 12 October 2012; revised 15 January 2013; accepted 16 January 2013; published online 21 February 2013

The rhizobium–legume symbiosis is a paradigm to address such questions. Legumes and soil bacteria collectively known as rhizobia have coevolved a mutualistic endosymbiosis of major ecological importance that contributes *ca* 25% of global nitrogen cycling (Masson-Boivin *et al.*, 2009). Rhizobia elicit on legume roots —occasionally stems— the formation of specialized organs called nodules in which they fix nitrogen to the benefit of the plant. In most present symbioses rhizobia massively infect nodule cells forming intracellular structures called symbiosomes (Gibson *et al.*, 2008; Ivanov *et al.*, 2010), although infection processes regarded as more primitive are also encountered (Sprent, 2001). Intracellular accommodation of rhizobia was an evolutionary quantum leap in the rhizobium–legume symbiosis as it boosted metabolic exchanges

between the two partners while shielding internalized bacteria, called bacteroids, from plant defense reactions. Which evolutionary forces drove the selection and maintenance of intracellular accommodation, a relatively late event in the symbiotic process, is so far unknown.

Experimental evolution that allows the identification of possible evolutionary pathways and mechanisms *via* a gain of function approach (Buckling *et al.*, 2009; Brockhurst *et al.*, 2011), is a powerful tool to tackle the evolution of symbiotic functions in rhizobia, which imposes facing considerable selective pressures such as plant immunity and nutrition. Rhizobia are phylogenetically disparate bacteria distributed in many genera of α- and β-proteobacteria intermixed with saprophytes and pathogens from which they may have evolved (Bontemps *et al.*, 2010; Sachs *et al.*, 2011). A bulk of evidence indicates that the large phylogenetic diversity of rhizobia originates from repeated and independent events of lateral gene transfer (LGT) of key symbiotic functions carried by plasmids or islands to non-symbiotic bacterial recipient genomes (Sullivan and Ronson, 1998; Rogel *et al.*, 2001; Ramsay *et al.*, 2006, 2009). Nodulation genes notably bring the capacity to synthesize morphogenic Nod factors signals that trigger the plant developmental program required for root hair infection and nodule organogenesis (Gough and Cullimore, 2011; Oldroyd *et al.*, 2011). Symbiotic traits have been disseminated over large phylogenetic distances as extant rhizobial lineages diverged long before they acquired symbiotic properties (Turner and Young, 2000), that is, after legumes appeared on earth 60 million years ago (Sprent, 2007). In the many cases where the donor and recipient bacteria were phylogenetically or genetically distant, expression of the symbiotic potential brought by LGT may have required genomic remodeling (Masson-Boivin *et al.*, 2009; Marchetti *et al.*, 2010).

In a previous study, we launched the experimental conversion of a soil bacterium into a legume symbiont by using *Cupriavidus taiwanensis* and *R. solanacearum* as symbiotic gene provider and recipient, respectively (Marchetti *et al.*, 2010). *C. taiwanensis* is a nitrogen fixing symbiont of *Mimosa pudica*. As most rhizobia, it invades host roots by means of root hair infection threads (ITs), which are initiated from micro-colonies entrapped within curled root hairs (Chen *et al.*, 2003). Extending and ramifying ITs bring bacteria to the root cortex where nodules are simultaneously developing (Gage, 2004; Oldroyd *et al.*, 2011). Bacteria are then released within target nodule cells (Ivanov *et al.*, 2010), where they divide ultimately leading to thousands of symbiosomes per cell. *R. solanacearum* is a phylogenetically distant plant pathogen of over 200 species that invades roots extracellularly (Genin, 2010). We mimicked the initial LGT event by introducing the symbiotic plasmid (0.5 Mb) of *C. taiwanensis* LMG19424 into *R. solanacearum* GMI1000, generating a non-nodulating *Ralstonia* chimera, CBM124. Following one cycle of massive inoculation, three spontaneous variants had gained the ability to nodulate *M. pudica*. Two of them were both nodulating and intracellularly infective. Intracellular infection capacity was acquired concomitantly to the nodulation capacity, upon inactivation of the master virulence regulator *hrpG*. The third clone, however, CBM356, induced ITs and nodules that were only extracellularly infected, upon inactivation of the type three secretion system (T3SS) (Marchetti *et al.*, 2010). We took advantage of this latter biological material to specifically explore the dynamics and genetics of acquisition of intracellular infection. Here, we report on the experimental evolution of CBM356 into nodule intracellular endosymbionts using serial plant bacterial coculture cycles. We identified new adaptive mutations for intracellular infection that were genetically and functionally different from *hrpG* inactivation, and contingent to the initial $T3SS^-$ nodulation-conferring mutation. This allowed us to investigate the relationships between nodulation and intracellular infection acquisition.

Materials and Methods

Bacterial strains, plasmids and growth conditions

Bacterial strains and plasmids used in this work are listed in Supplementary Table S1. *R. solanacearum* strains were grown at 28 °C on rich peptone broth rich medium (BG) medium supplemented with 28 mM glucose (Boucher *et al.*, 1985). Antibiotics were used at the following concentrations (in micrograms per milliliter): spectinomycin 40, trimethoprim 100, tetracycline 10, gentamicin 10, chloramphenicol 12.5 and kanamycin 25.

Generation of symbiotically evolved clones and populations

The ancestral strain CBM356 grown overnight in peptone broth rich medium supplemented with trimethoprim was inoculated to three sets of 30 *M. pudica* plants (three plants per tube). Bacteria (10^7) per tube were used as inoculum. Twenty-one days after inoculation, all nodules from each set of 30 plants were pooled, sterilized with 2.6% sodium hypochlorite during 15 min and crushed. Ten percent of the nodule crush was used to inoculate the same day a new set of 30 plants. Three independent and parallel lineages of 16 cycles of inoculation-isolation of nodule bacteria were generated in this way. The use of 30 plantlets per cycle may minimize the effect of plant individual variability. At each cycle, serial dilutions of each nodule crush were plated and one clone was randomly selected from the highest dilution and purified. The selected clones, the rest of the nodule crushes and a 48-h culture of bacteria from an aliquot of nodule crushes

were stored at −80 °C. When the total number of recovered nodule bacteria was below 10^5, 10^6–10^7 bacteria from the 48-h culture were added per tube of plants 3 days after inoculation with the nodule crush. This happened for cycles M3, M4, M7, M15, N2–4, N6–8, N10–11, and S2–9.

Plant assays and cytological studies

Seedlings of *M. pudica* were grown in Gibson tubes under N-free conditions as previously described (Marchetti *et al.*, 2010). For nodulation kinetics, 10 plants (1 plant/tube) were inoculated with 10^4 bacteria per plant. Two independent experiments were performed. For cytological analyses, nodules were harvested at 14 dpi, fixed in glutaraldehyde and treated as previously described (Marchetti *et al.*, 2010) for either 1 µm ultrathin or 60-µm thick sections. LacZ-tagged infecting bacteria were stained following the standard procedure as described (Marchetti *et al.*, 2010). The number of infected cells per nodule section was estimated on the largest section of each nodule. In each experiment, nodules were collected from 10 tubes of plants. For competition experiments, plants were coinoculated with $10^4/10^4$ (ratio 1/1) or $10^4/10^6$ (ratio 1/100) cells of two different strains. About 100 nodules were collected and sterilized 21 days after inoculation. Surface-sterilized nodules were individually crushed and plated on selective medium for nodulation competitiveness analysis (estimated by the number of nodules formed by each clone). For *in planta* fitness analysis (estimated by the number of each clone in the whole-nodule population), all surface-sterilized nodules were pooled, crushed and plated on selective medium. For rhizoplane colonization, three tubes containing two plants were coinoculated with $10^5/10^5$ cells of two different clones (inoculum ratio 1/1). Fourty-eight hours after inoculation, each root was transferred into 10 ml of sterile water and strongly vortexed. Recovered bacteria, detached from the root, were diluted and plated on selective medium. The remaining plant culture medium was centrifuged 15 min at 4000 r.p.m., resuspended in 1 ml of sterile water, diluted and plated on selective medium. Two independent experiments were performed. In all coinoculation experiments, inoculum ratios were verified by plating serial dilutions of inocula on selective medium.

Statistical analyses

All statistical analyses were performed using the R software. Multiple comparisons to assess differences in fitness and number of infected cells were performed using the non-parametric statistical test of Kruskal–Wallis with a *P*-value threshold of 0.05. Comparisons were done among evolved clones belonging to the same lineage and the corresponding reconstructed mutants taken either the last extracellular infective clone or the first intracellular infective clone as reference.

Other materials and methods concerning the construction of mutants, the analysis of mutation fixation rates, pathogenicity and β-glucuronidase assays are described in Supplementary Information. Primers used in this study are listed in Supplementary Table S2.

Results

Evolution of intracellularly infectious clones from an extracellular Ralstonia nodulating ancestor

CBM356, a spontaneous *M. pudica*-nodulating derivative of the chimeric *Ralstonia* CBM124 (Figure 1a), formed on *M. pudica* a few abnormal nodules that were poorly and only extracellularly invaded (Marchetti *et al.*, 2010) (Figures 1c and 2). To improve its infection capacity, CBM356 was progressively adapted to nodule tissues by serial *in planta* passages. In brief, cultured bacteria were first inoculated to *M. pudica* seedlings. Twenty-one days after, bacteria were isolated from nodules and directly reinoculated on new plants. Sixteen successive cycles of plant inoculation/nodule bacteria isolation were performed three times independently (see Materials and Methods), generating three parallel lineages, M, N and S (Figure 1a). Bacteria serving as inocula at each cycle came from ITs and extracellular spaces, as well as from nodule cells if an intracellularly infecting sub-population emerged along the experiment. Noteworthy, *C. taiwanensis* bacteroids are not terminally differentiated in *M. pudica* nodules (Marchetti *et al.*, 2011), that is, do not lose their ability to reproduce and thus to re-enter into symbiosis, in contrast to symbionts of legumes of the galegoid clade (Mergaert *et al.*, 2006). This selection regime may favor the fixation of beneficial mutations improving nodulation, that is, allowing bacteria to produce more nodules, or infection, that is, allowing bacteria to reach higher density in nodules, along the experiment. In principle, infection could be improved either via increased extracellular infection or intracellular infection acquisition.

In contrast to the CBM356 ancestor, the three final evolved clones M16, N16 and S16 were all capable of intracellular infection, although with different efficiencies (Figures 1b and d–f). Nodule cell infection capacity was however lower than that of the reference *M. pudica* symbiont, *C. taiwanensis* (Chen *et al.*, 2003). Indeed, less bacteria were routinely isolated per nodule (Figure 2), there is a larger variance in number of infected nodule cells (Figure 1b) and of recovered bacteria (Figure 2) and the nodules did not fix nitrogen.

Changes in infection ability along the three lineages were monitored by semiquantitative cytological observations of nodules induced by individual clones from intermediate evolved populations.

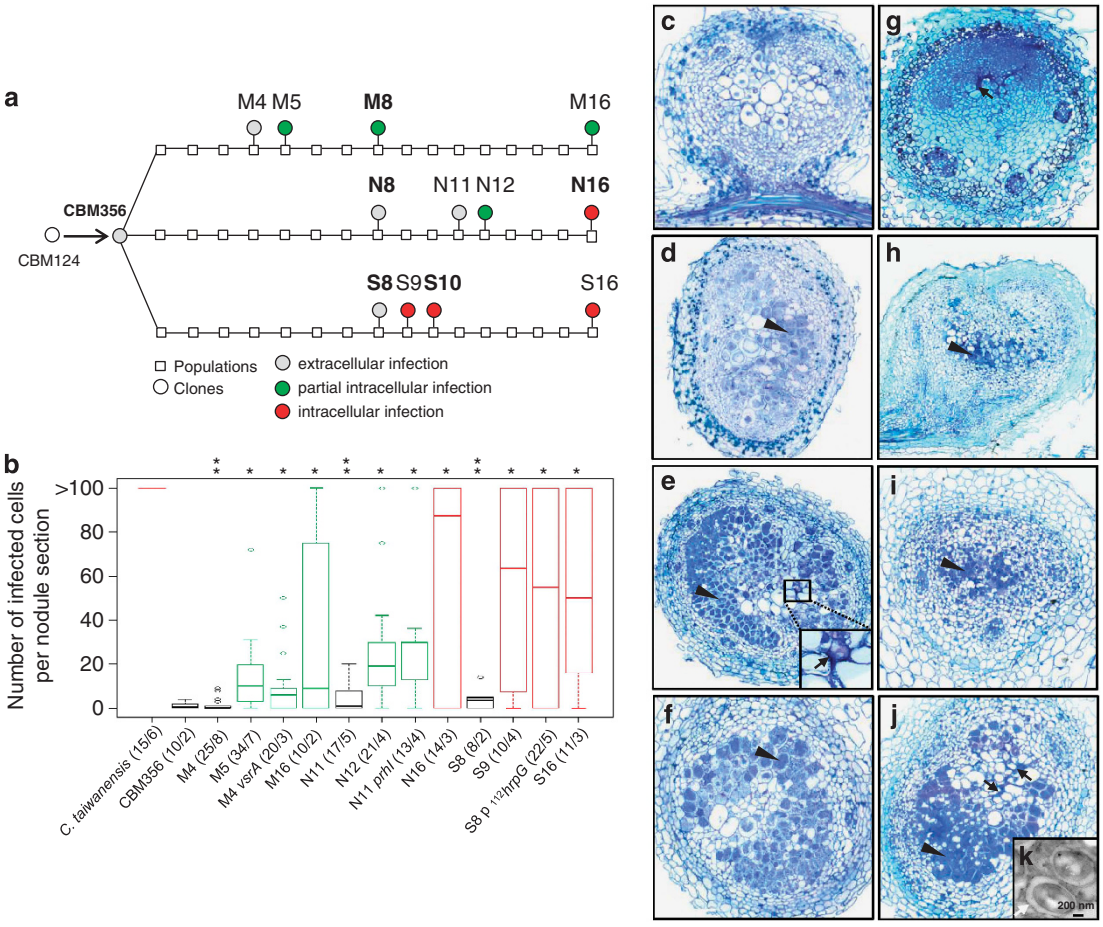

Figure 1 Evolution of intracellularly infectious *Ralstonia* clones. (**a**) Three independent lineages (M, N, S) were derived from CBM356, a spontaneous *M. pudica*-nodulating derivative of the chimeric *Ralstonia* CBM124 (Marchetti *et al*., 2010). Clones completely resequenced are in bold. Color code is as in **b**. (**b**) Box-plots representing the distribution of the number of infected cells per section of nodules. The central rectangle spans the first quartile to the third quartile (i.e., the interquartile range *or* IQR), the bold segment inside the rectangle shows the median, unfilled circles indicate suspected outliers, whiskers above and below the box show either the locations of the minimum and maximum in the absence of suspected outlying data or 1.5 × IQR if outliers are present. Numbers in parentheses indicate the number of nodules analyzed (8–34) and the number of independent experiment (2–8) performed for each strain. In black, green and red are strains with a median number of infected cells per section below 5, between 5 and 50, and above 50, respectively. Single stars indicate significant differences with the last extracellular clones, either M4, N11 or S8, and double stars indicate significant differences with the first intracellular infective clones, either M5, N12 or S9 ($P<0.05$; multiple comparison test after Kruskal–Wallis). (**c–j**) Toluidine blue staining of 1 μm sections of *M. pudica* nodules induced by the ancestor CBM356 (**c**), the final clones M16 (**d**), N16 (**e**) and S16 (**f**) and the reconstructed mutants CBM125 (*hrcV*) (**g**), CBM1619 (*hrcS vsrA*) (**h**), RCM51 (*hrcS prhI*) (**i**) and RCM55 (*hrcV* p^{112}*hrpG*) (**j** and **k**). In the intracellularly infected zone (arrowhead), nodule cells are full of bacteroids (in blue). Intracellular bacteria were surrounded by a peribacteroid membrane (white arrow) forming symbiosomes (**k**). Black arrows, intercellular bacteria.

A *lacZ* fusion (pCBM01) constitutively expressed in nodules was introduced in selected clones. These strains were then inoculated onto *M. pudica* seedlings and the nodule sections were analyzed with respect to infection 14 days after inoculation. Shifts in infection ability from predominantly extracellular to predominantly intracellular infection were observed between clones M4/M5, between N11/N12, and between S8/S9 (Figure 1b and Supplementary Figure S1). The level of nodule infection, as assessed by plating nodule crushes or *in planta* fitness (Figure 2), showed a 1–2 log increase in the number of bacteria per nodule between N11/N12 and between S8/S9. M5 instead had a limited infection capacity (Figure 2). We thus identified three shifts in infection capacity that occurred with different efficiencies in the M, N and S lineages, in the 5th, 9th and 12th cycles of the evolution experiment, respectively (that is, after *ca* 125, 225 and 300 generations, respectively).

Identifying the mutations that drove the transition from extracellular to intracellular infection

To map the mutations associated with the phenotypic shifts, we took advantage of the resequencing of some intermediate and final clones, i.e., M8, N8, N16, S8 and S10. Sequence data were mapped to the ancestral reference genome (6.37 Mb) based on the known genome sequences of *R. solanacearum*

GMI1000 (Salanoubat *et al*., 2002) and *C. taiwanensis* LMG19424 (Amadou *et al*., 2008) and analyzed using the SNiPer 1 software (Marchetti et al., 2010). In a first step we compared M8 with CBM356, N16 with N8 and S10 to S8 for the presence of non-synonymous and intergenic mutations. In a second step we identified among them those present in clones M5, N12 and S9 and absent in previous clones using PCR amplification and Sanger sequencing of DNA regions surrounding the detected mutations. In all three cases, we found one mutation that affects a regulatory gene of the virulence pathway of *R. solanacearum* (Table 1) (see Figure 3a for a partial view of the complex virulence pathway). Frameshift mutations in genes encoding the histidine kinase *vsrA* and the sigma factor *prhI*

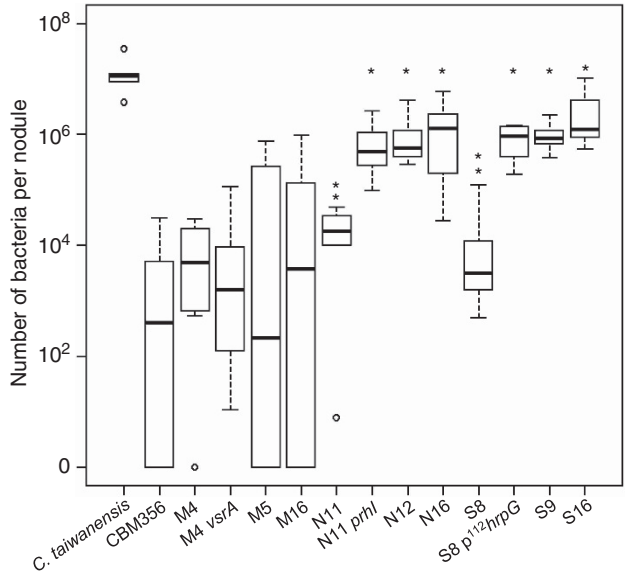

Figure 2 Fitness of *C. taiwanensis*, evolved clones and reconstructed mutants. Box-plots represent the distribution of the number of bacteria per nodule recovered at 21 dpi. The central rectangle spans the first quartile to the third quartile (that is, the interquartile range or IQR), the bold segment inside the rectangle shows the median, unfilled circles indicate suspected outliers, whiskers above and below the box show either the locations of the minimum and maximum in the absence of suspected outlying data or 1.5 × IQR if an outlier is present. Data correspond to 6–12 measures obtained from 2 to 4 independent experiments for each strain. Single stars indicate significant differences with the last extracellular clones, either M4, N11 or S8, and double stars indicate significant differences with the first intracellular infective clones, either M5, N12 or S9 ($P<0.05$; multiple comparison test after Kruskal–Wallis).

were observed in clones M5 and N12, respectively, while a single-nucleotide change was detected in the promoter region of *hrpG* (mutation referred as to p^{112}*hrpG*) in clone S9 (Supplementary Figure S2c). We confirmed that the *vsrA*, *prhI* and p^{112}*hrpG* mutations actually affected pathogenicity of the wild-type chimeric ancestor CBM124 (Supplementary Figures S2a and S2b).

To assess the possible role of these mutations in intracellular infection acquisition in the evolution experiment, we inactivated *vsrA* and *prhI*, and reconstructed the p^{112}*hrpG* mutation in clones M4, N11 and S8, respectively, as well as in the ancestral *Ralstonia* background (CBM124) bearing a nodulation-conferring T3SS$^-$ (*hrcV* or *hrcS*) mutation. The *prhI* and p^{112}*hrpG* mutants induced nodules that were predominantly intracellularly infected (Figures 1b, i and j and Supplementary Figure S1) and that contained high amounts of bacteria comparable to those induced by the intracellularly infective clones N12 and S9, respectively (Figure 2). Infected cells housed typical symbiosomes composed of internalized bacteria surrounded by a peribacteroid membrane (Figure 1k and Supplementary Figure S3). The intracellular zone was however not always fully developed and often still associated with a limited zone of extracellular infection (Figure 1j). M4 *vsrA* induced partial intracellular infection (Figure 1b and Supplementary Figure S1). However, no statistically significant difference in the number of nodule bacteria was obtained between M4 *vsrA*- and CBM356-induced nodules (Figure 2). Thus, unlike *prhI* and p^{112}*hrpG*, *vsrA* had a weak effect on intracellular infection.

Interestingly, when reconstructed in the wild-type chimeric strain CBM124, none of the three mutations, *vsrA*, *prhI* or p^{112}*hrpG*, however conferred the ability to both nodulate and intracellularly infect *M. pudica*. A CBM124 *vsrA* mutant was unable to nodulate (Figure 4a). Although the CBM124 *prhI* and CBM124 p^{112}*hrpG* mutants were able to nodulate (Figure 4a), nodules formed by these two single mutants were not intracellularly invaded (Figures 4b and c), contrary to nodules induced by the double *hrcS* (T3SS$^-$)-*prhI* and *hrcV* (T3SS$^-$)-p^{112}*hrpG* mutants (Figures 1i and j). This showed that the three adaptive mutations that were selected in the CBM356-derived lineages are contingent on the initial nodulation-conferring *hrcV* (T3SS$^-$)

Table 1 Mutations altering a virulence regulatory gene and conferring intracellular infection ability

Clone	*Position*	*GeneID*	*Description*	*Distance to the flanking gene*	*Mut*	*Protein modification*
M5	322207	RSc0289	*vsrA* Transmembrane sensor kinase		C/–	Frameshift
N12	1080278	RSp0849	*prhI* Sigma factor, transcription regulator		C/–	Frameshift
	1080280	RSp0849	*prhI* Sigma factor, transcription regulator		G/T	C5F
S9	1083412[a]	RSp0852	*hrpG* Transcription regulator	112	G/A	

[a]Mutation located in the intergenic region upstream of the gene indicated.

mutation. Moreover, this showed that the T3SS blocks intracellular infection in addition to root hair entry and nodulation (Figure 3a). Interestingly, at both entry points (that is, root hair and nodule cell) the cell wall is locally degraded and bacteria come into close contact with the cell membrane.

Adaptive mutations involved in intracellular infection acquisition confer increased nodulation capacity

To identify which selection forces drive the emergence and fixation of a population able to invade and thrive in the intracellular environment, we followed the fixation rates of the *vsrA*, *prhI*, and p^{112}*hrpG* mutations in evolved populations bordering the phenotypic shifts. DNA fragments surrounding the mutations sites were amplified by PCR on evolved populations and sequenced using the Roche 454 technology (Table 2). The *vsrA* mutation was already present in the M2 population and progressively increased until reaching *ca* 100% of the allele frequency in the M6 population. The *prhI* and p^{112}*hrpG* mutations first appeared in populations N12 and S9, where they represented 85 and 90% of the nucleotide polymorphism. The fact that, in the N and S lineages, clones bearing an adaptive mutation for intracellular infection were undetected in the inoculum and present at an extremely high level in the nodule population suggested that the *prhI* and p^{112}*hrpG* mutations conferred a selective advantage for nodulation or were associated with a mutation improving nodulation competitiveness. Coinoculation experiments revealed that inactivation of *prhI* or reconstruction of p^{112}*hrpG* conferred to the extracellularly infectious clones N11 and S8, respectively, a strong competitive advantage for nodulation (Table 3). Indeed, even when the mutated clones represented only 1% of the inoculum, they formed 35–59% of the nodules. Higher competitiveness effect did not originate from an increased colonization of the culture medium or the rhizoplane (Supplementary Figure S4) as assessed by bacteria counting in these two environments. By contrast, we observed a strong impact of the mutations on nodulation itself. The *prhI* and p^{112}*hrpG* mutations were indeed found to greatly improve the nodulation kinetics of a chimeric *Ralstonia* bearing a T3SS$^-$ (*hrcV* or *hrcS*) mutation allowing the induction of 4–5 times more nodules at 21 days post inoculation (dpi)

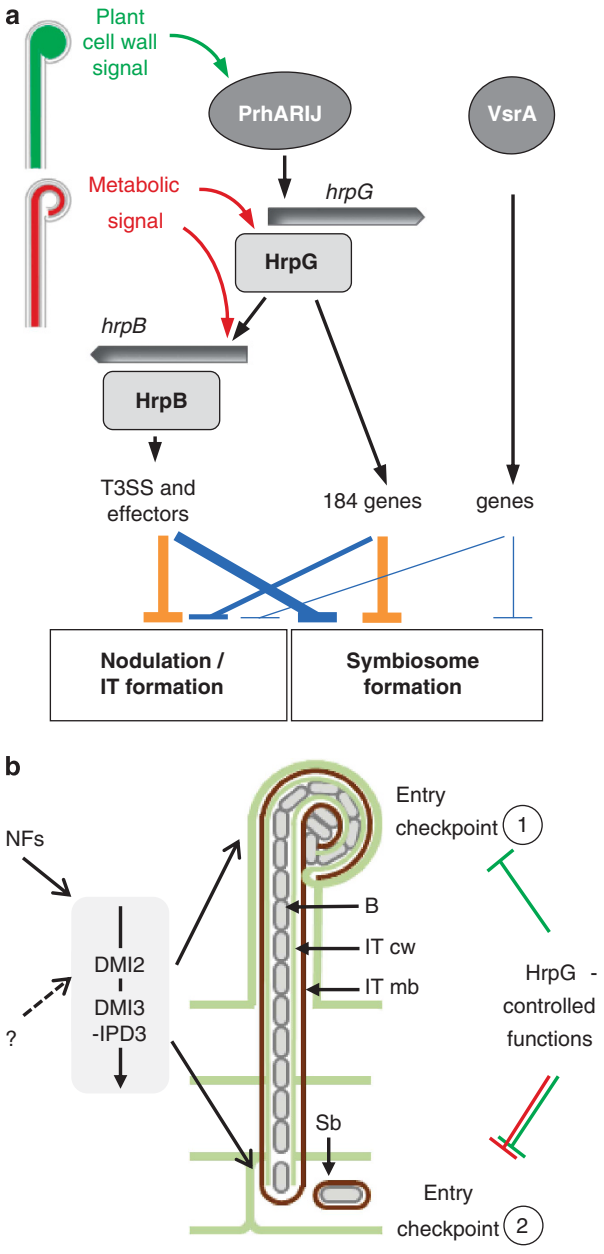

Figure 3 Effect of the *R. solanacearum* virulence pathway on symbiosis and proposed model for the HrpG-dependent control of root hair and nodule cell entry. (**a**) PrhARIJ-based plant cell contact activation of *hrpG* (symbolized in green) involves a constitutive and ubiquitous component of the cell wall and thus likely occurs in the infection site and within the IT, where bacteria are in contact with the root hair wall and the IT wall, respectively. HrpG post-transcriptional modification and activation of *hrpB* transcription (symbolized in red) by an unidentified environmental metabolic signal(s) (Genin *et al.*, 1992; Brito *et al.*, 1999; Plener *et al.*, 2010) likely occurs in the IT apoplastic medium. No link between the sensor histidine kinase VsrA and HrpG has been evidenced so far. Mutation effects on symbiotic properties symbolized by orange lines were previously shown (Marchetti *et al.*, 2010), while effects symbolized by blue lines were evidenced in this study. The thickness of the line symbolizes the strength of the interference. (**b**) In the root hair curl ①, the *prh* cascade is activated, blocking early entry and nodulation. Nodulation occurs with either a T3SS, *hrpG* or *prh* cascade mutant. Within cell-wall-bound ITs ②, the *prh* cascade, the *hrpB* transcription and the post-transcriptional modification of HrpG are induced, blocking intracellular infection. Intracellular infection occurs with either a *hrpG* or a double T3SS and *prh* cascade mutant. In this latter double mutant, activation of the 184 HrpG-controlled genes via post-transcriptional modification of HrpG may not be sufficient to block intracellular infection. DMI2 and the DMI3 interacting protein IPD3, which are part of the plant signaling pathway induced by rhizobial Nod factors, are involved in nodule and IT formation and have a role in symbiosome formation. B, bacteria; cw, cell wall; mb, membrane; Sb, symbiosome.

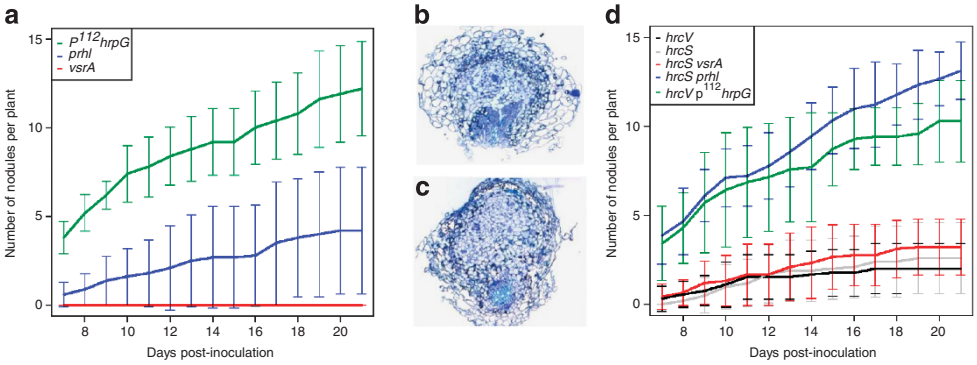

Figure 4 Effect of the *prhI* p[112]*hrpG* and *vsrA* mutations on the nodulation kinetics and infection phenotype of *Ralstonia* chimera. (**a**) Nodulation kinetics of the single mutants CBM124 *prhI*, CBM124 p[112]*hrpG* and CBM124 *vsrA*. Values are from one representative experiment. (**b**, **c**) Toluidine blue staining of 1 μm ultrathin sections of 14-day-old *M. pudica* nodules induced by CBM124 *prhI* (**b**) and CBM124 p[112]*hrpG* (**c**). (**d**) Nodulation kinetics of double *hrcS vsrA*, *hrcS prhI* and *hrcV* p[112]*hrpG* mutants of CBM124. HrcS and HrcV are structural components of the T3SS pilus. Values are from one representative experiment.

Table 2 Dynamics of fixation of the *vsrA*, *prhI* and p[112]*hrpG* mutations in evolved populations

Mutations	*Populations*				
vsrA	*M2*	*M3*	*M4*	*M5*	*M6*
Number of reads	3191	2808	4509	6210	6122
% of mutated sequences	0.9	11.8	21.2	89.1	99.6
prhI	*N10*	*N11*	*N12*	*N13*	
Number of reads	4004	2200	1480	2626	
% of mutated sequences	0	0.04	85.2	99.2	
p[112]*hrpG*	*S7*	*S8*	*S9*	*S10*	
Number of reads	612	1004	943	1165	
% of mutated sequences	0.4	0.1	89.9	97.2	

Mutation frequencies were calculated by resequencing regions surrounding the mutations using GS FLX 454.
Mutation frequencies in populations N10, N11, S7 and S8 were below the level of detection of the method.

(Figure 4d). HrpG was previously shown to control nodulation in a T3SS-dependent manner. It thus appeared here that HrpG also controls T3SS-independent functions that affect nodulation (Figure 3a).

In coinoculation experiments (Table 3) *prhI* and p[112]*hrpG* mutations had a huge effect on the *in planta* fitness of the strains that could not be explained solely by their impact on nodulation competitiveness indicating that their very quick fixation in the lineages originated from their impact on both nodulation and *in planta* bacterial multiplication.

The *vsrA* mutation, which had a weak effect on intracellular infection, also had a weak effect on nodulation (Figure 4d and Table 3), confirming the correlation between nodulation and intracellular infection capacity levels observed with the *prhI* and p[112]*hrpG* mutants.

Discussion

Exchange of genetic material, which is favoured within the same ecological niche (Smillie *et al.*, 2011), has a major role in bacterium evolution (Dagan and Martin, 2007). Although LGT is a crucial start point for the spread of genetic innovation in nature (Ochman and Moran, 2001), the full phenotypic expression of the acquired traits often requires readjustment of the new genetic background, especially when the phylogenetic or functional distance between recipient and donor cells is large (Popa and Dagan, 2011). How recipient genomes rewire to express adaptive traits that operate profound changes in their lifestyle is largely unknown. The rhizobium–legume symbiosis is an excellent biological system to address this issue.

Here, we have pursued the previously launched evolution experiment of the plant pathogen *Ralstonia solanacearum* into a legume symbiont by submitting a nodulating but only extracellularly infectious *R. solanacearum*-derived clone (CBM356) to serial *in planta* (*M. pudica*) passages by using an experimental protocol that reasonably mimicked natural events. In nature indeed, when nodules senesce, bacteria are released in the soil where they survive and reproduce until their progeny infects a new legume host. Noteworthy, rhizobial sub-populations that colonize the rhizosphere of a given seedling in the field may originate from different previously grown individual plants. In our laboratory conditions, the three CBM356-derived lineages acquired intracellular infection capacity with different dynamics and efficiency, yet in <11 cycles, that is, *ca* 300 generations, revealing that the legume represents a highly selective environment for the evolution of this trait, as for nodulation (Marchetti *et al.*, 2010; Crook *et al.*, 2012).

Acquisition of intracellular infection capacity during experimental evolution was associated with mutations targeting regulators of the virulence pathway of the recipient genome, strongly

Table 3 Competition for nodulation and relative fitness of the poorly infective evolved clones M4, N11 and S8 coinoculated with their respective infective mutants M4 *vsrA*, N11 *prhI* and S8 p[112]*hrpG*

Competition mix A/B	*Inoculum*		*Competition for nodulation*				*Relative fitness*		
	% of bacteria		*% of nodules*			*CI*[a] *(A/B)*	*% of bacteria in nodule population*		*CI*[a] *(A/B)*
	A	*B*	*A*	*B*	*Empty*		*A*	*B*	
M4 *vsrA*/M4	55 ± 20	45 ± 20	40 ± 14	10 ± 14	50 ± 14	11.5 ± 14	nd	nd	nd
M4 *vsrA*/M4	19 ± 5	81 ± 5	17 ± 6	39 ± 6	44 ± 10	1.9 ± 0.1	43 ± 20	57 ± 20	3.6 ± 2.2
M4 *vsrA*/M4	7 ± 1	93 ± 1	24 ± 16	19 ± 1	57 ± 18	17 ± 10	36 ± 15	64 ± 15	9.3 ± 7.3
N11 *prhI*/N11	50 ± 4	50 ± 4	84 ± 6	3 ± 2	13 ± 4	36 ± 15	nd	nd	nd
N11 *prhI*/N11	2 ± 0.6	98 ± 0.6	59 ± 10	23 ± 4	18 ± 14	141 ± 117	96 ± 2	4 ± 2	1571 ± 806
S8 p[112]*hrpG*/S8-SpeR[b]	46 ± 2	54 ± 2	92 ± 1	2 ± 2	6 ± 1	30 ± 13	nd	nd	nd
S8 p[112]*hrpG*/S8-SpeR[b]	1 ± 0.4	99 ± 0.4	35 ± 5	25 ± 5	40 ± 10	236 ± 146	99.7 ± 0.4	0.3 ± 0.4	166 164 ± 175 121
S8-SpeR[b]/S8	47 ± 0.7	53 ± 0.7	32 ± 1.5	33 ± 2.5	36 ± 3.9	1.5 ± 0.7	nd	nd	nd

Values are averages ± s.d. ($n = 3$).
[a]Competitive index, CI (A/B) for competitiveness = (% nodules induced by A/% A in inoculum)/(% nodules induced by B/% B in inoculum), CI (A/B) for relative fitness = (% A in nodule population/% A in inoculum)/(% B in nodule population/% B in inoculum).
[b]The GenR cassette was replaced by a SpeR cassette in S8 to allow strain identification on the basis of antibiotic resistance.

suggesting that several virulence-associated functions interfere with symbiosome formation. The *R. solanacearum* virulence network is orchestrated by the central regulator HrpG that controls a type III secretion machinery (T3SS) and associated effectors via the intermediate regulator HrpB (Poueymiro and Genin, 2009), as well as many genes involved in virulence and host adaptation via a still unknown circuitry (Valls *et al.*, 2006) (Figure 3). *hrpG* is activated by plant cell contact through the PrhARIJ cascade (Aldon *et al.*, 2000). In addition, HrpG-controlled functions can also be activated via HrpG post-transcriptional modification, as well as via activation of *hrpB* transcription by an unidentified environmental metabolic signal(s) perceived in minimal culture medium (Genin *et al.*, 1992; Brito *et al.*, 1999; Plener *et al.*, 2010). Beside HrpG, the sensor histidine kinase VsrA controls many other virulence functions (Schell *et al.*, 1994; Huang *et al.*, 1995; Schneider *et al.*, 2009; Meng *et al.*, 2011). In a previous study we showed that a *hrpG* stop mutation allowed the chimeric *Ralstonia* to infect nodule cells, via the modulation of T3SS-independent HrpG-controlled functions (Marchetti *et al.*, 2010). Here, we identified three new mutations —one per lineage— required for intracellular infection, which genetically and functionally differ from a *hrpG* stop mutation. A mutation inactivating *vsrA* had a weak effect on intracellular infection activation, while two mutations targeting the activation pathway of HrpG (*prhI*, p[112]*hrpG*) converted an extracellularly infecting chimeric *Ralstonia* into a predominantly intracellular legume symbiont. One-hundred and eighty four genes are controlled by HrpG in a HrpB-independent way (Valls *et al.*, 2006), encoding functions such as plant cell-wall degradation, virulence determinants or phytohormone production. Which HrpG-controlled functions negatively impact on intracellular infection remains to be elucidated.

The effect on infection of these three mutations was found to be contingent on the initial *hrcV* (T3SS$^-$) mutation carried by the CBM356 ancestor, reinforcing previous evidence that evolution is thrifty (Pelosi *et al.*, 2006). The *vsrA* mutation alone did not allow the wild-type chimera CBM124 to nodulate, in agreement with the fact that *vsrA* does not control the T3SS. More unexpected was the observation that individual reconstruction of *prhI* or p[112]*hrpG* mutations conferred to the wild-type chimera the ability to nodulate—likely via T3SS inactivation at the root entry stage (Figure 3)— but not to infect nodule cells. Intracellular infection was restored by adding a T3SS$^-$ mutation, indicating that the T3SS blocks intracellular infection, in addition to nodulation (Marchetti *et al.*, 2010). T3SS reactivation within ITs in *prhI* and p[112]*hrpG* mutants is likely due to both the post-transcriptional activation of HrpG (Brito *et al.*, 1999) and the transcriptional activation of *hrpB* (Genin *et al.*, 1992; Plener *et al.*, 2010) by a metabolic signal present in the IT apoplastic fluid (Figure 3a). Rhizobia were shown to use T3SS to promote or impair symbiosis upon secretion of type three effectors that often have homologs in pathogenic bacteria (Deakin and Broughton, 2009). Known negative effects of rhizobial T3SS include alteration of root hair infection and nodule formation (Chatterjee *et al.*, 1990), nodule infection (Hubber *et al.*, 2004) or symbiosome differentiation (Yang *et al.*, 2010). Thanks to the dual regulation of HrpG, our work showed that T3SS can block both root hair and intracellular infection on the same host plant.

Here, we showed that the adaptive mutation allowing nodulation/IT formation and those activating intracellular infection actually impacted on both

processes at a similar level (Figure 3). In addition to providing evidence that the T3SS also blocks symbiosome formation, we showed that significant activation of the late symbiotic event of nodule intracellular infection occurred during the evolution experiment *via* mutations (*prhI*, p^{112}*hrpG*) that were actually selected for their impact on nodulation competitiveness, that is, the ability of bacteria to compete successfully for nodulation and root hair entry on the host plant, while they were likely fixed in the evolving populations by their cumulative effect on nodulation and *in planta* multiplication. These two adaptive mutations had a strong positive impact on both nodulation competitiveness and kinetics, likely by improving root hair entry, a limiting trait of nodulation efficiency. IT formation is indeed linked to nodule organogenesis, both of which are under the control of rhizobial Nod factors that trigger the symbiotic plant developmental programs (Gough and Cullimore, 2011). Whether the same T3SS effector(s) or the same HrpG-controlled functions interfere with both the early and late symbiotic events still remain to be determined. The late symbiotic event of nodule cell infection is tightly coupled to nodulation, rendering its specific analysis difficult. A genetic link between nodulation/IT formation and nodule cell infection was also evidenced on the plant side as two genes of the Nod factor signaling pathway, the leucine-rich-repeat-containing receptor kinase DMI2 and the calcium-and calmodulin-dependent kinase DMI3 interacting protein IPD3, were shown to be required for symbiosome formation (Capoen *et al.*, 2005; Limpens *et al.*, 2005; Ovchinnikova *et al.*, 2011). Our findings on the bacterial side provide new clues on nodulation-intracellular infection relationships by pointing to a common control for bacterial invasion at the early nodulation/root hair infection and the late nodule cell entry levels (Figure 3b). In our system, nodule cell invasion however appeared more stringent than nodulation, as the former requires the inactivation of the T3SS and of unknown T3SS-independent functions, while the latter occurs —although poorly— in a T3SS single mutant.

The post-LGT bacterial coupling of intracellular infection to nodulation evidenced in our system may have major evolutionary implications. The strong impact of intracellular infection on nodulation competitiveness sounds biologically very meaningful in respect to the dissemination of legume symbionts in phylogenetically disparate bacteria. In our experimental conditions, as well as in nature, very few nodules are formed per plant in comparison to the number of root colonizing bacteria. As a single bacterium enters and multiplies within nodules (Gage, 2002), any rhizospheric bacterium has a very remote chance to invade the root if it is not highly competitive for nodulation/initial infection. The coupling of the bacterial abilities to nodulate and infect nodules intracellularly may thus have favored the spread and maintenance of intracellular infection capacity in nodulating bacteria and, conversely, have generated a positive selection pressure on nodulation genes by increasing bacterial fitness *in planta*. This may explain why rhizobia inducing intercellularly invaded nodules have never been described, to our knowledge, in nature.

Diverse modes of root infection —direct intercellular infection, crack entry and root hair infection— and nodule cell infection —modified ITs called fixation threads and symbiosomes— are encountered in extant legumes, whose evolutionary relationships is still not fully understood (Sprent, 2007). Root hair infection was shown to be the most controlled entry process and proposed to be the most highly evolved mode of root invasion in legumes (Madsen *et al.*, 2010), while symbiosome accommodation that does not occur in all symbioses (Sprent, 2007) is considered as the most evolved nodule cell infection process. Our work provides support to similar requirements at both root hair and nodule cell entry levels that we speculate to have favoured the coevolution of bacterial capacity to enter root hairs and nodule cells in the course of the legume–rhizobium evolution.

Acknowledgements

We are grateful to E Rocha and J Cullimore for comments and M Marchetti for help in cytological work. This work is part of the 'Laboratoire d'Excellence' (LABEX) entitled TULIP (ANR -10-LABX-41) and is supported by grants from SPE INRA and ANR-08-BLAN-0295-01. Roche GS FLX 454 sequencing was performed at the PlaGe Platform of the Toulouse Genopole. SHG and LT were supported by a fellowship from the China Scholarship Council and ANR-08-BLAN-0295-01, respectively.

References

Aldon D, Brito B, Boucher C, Genin S. (2000). A bacterial sensor of plant cell contact controls the transcriptional induction of *Ralstonia solanacearum* pathogenicity genes. *Embo J* **19**: 2304–2314.

Amadou C, Pascal G, Mangenot S, Glew M, Bontemps C, Capela D *et al.* (2008). Genome sequence of the beta-rhizobium *Cupriavidus taiwanensis* and comparative genomics of rhizobia. *Genome Res* **18**: 1472–1483.

Bontemps C, Elliott GN, Simon MF, Dos Reis Junior FB, Gross E, Lawton RC *et al.* (2010). *Burkholderia* species are ancient symbionts of legumes. *Mol Ecol* **19**: 44–52.

Boucher CA, Barberis PA, Trigalet AP, Demery DA. (1985). Transposon mutagenesis of *Pseudomonas solanacearum*—isolation of Tn5 induced avirulent mutants. *J Gen Microbiol* **131**: 2449–2457.

Brito B, Marenda M, Barberis P, Boucher C, Genin S. (1999). *prhJ* and *hrpG*, two new components of the plant signal-dependent regulatory cascade controlled by PrhA in *Ralstonia solanacearum*. *Mol Microbiol* **31**: 237–251.

Brockhurst MA, Colegrave N, Rozen DE. (2011). Next-generation sequencing as a tool to study microbial evolution. *Mol Ecol* **20**: 972–980.

Buckling A, Maclean RC, Brockhurst MA, Colegrave N. (2009). The Beagle in a bottle. *Nature* **457**: 824–829.

Capoen W, Goormachtig S, De Rycke R, Schroeyers K, Holsters M. (2005). SrSymRK, a plant receptor essential for symbiosome formation. *Proc Natl Acad Sci USA* **102**: 10369–10374.

Chatterjee A, Balatti PA, Gibbons W, Pueppke SG. (1990). Interaction of *Rhizobium fredii* USDA257 and nodulation mutants derived from it with the agronomically improved soybean cultivar McCall. *Planta* **180**: 301–311.

Chen WM, James EK, Prescott AR, Kierans M, Sprent JI. (2003). Nodulation of *Mimosa* spp. by the beta-proteobacterium *Ralstonia taiwanensis*. *Mol Plant Microbe Interact* **16**: 1051–1061.

Crook MB, Lindsay DP, Biggs MB, Bentley JS, Price JC, Clement SC *et al.* (2012). Rhizobial plasmids that cause impaired symbiotic nitrogen fixation and enhanced host invasion. *Mol Plant Microbe Interact* **25**: 1026–1033.

Dagan T, Martin W. (2007). Ancestral genome sizes specify the minimum rate of lateral gene transfer during prokaryote evolution. *Proc Natl Acad Sci USA* **104**: 870–875.

Deakin WJ, Broughton WJ. (2009). Symbiotic use of pathogenic strategies: rhizobial protein secretion systems. *Nature Rev Microbiol* **7**: 312–320.

Gage DJ. (2002). Analysis of infection thread development using Gfp- and DsRed-expressing *Sinorhizobium meliloti*. *J Bacteriol* **184**: 7042–7046.

Gage DJ. (2004). Infection and invasion of roots by symbiotic, nitrogen-fixing rhizobia during nodulation of temperate legumes. *Microbiol Mol Biol Rev* **68**: 280–300.

Genin S. (2010). Molecular traits controlling host range and adaptation to plants in *Ralstonia solanacearum*. *New Phytol* **187**: 920–928.

Genin S, Gough CL, Zischek C, Boucher CA. (1992). Evidence that the *hrpB* gene encodes a positive regulator of pathogenicity genes from *Pseudomonas solanacearum*. *Mol Microbiol* **6**: 3065–3076.

Gibson KE, Kobayashi H, Walker GC. (2008). Molecular determinants of a symbiotic chronic infection. *Annu Rev Genet* **42**: 413–441.

Gough C, Cullimore J. (2011). Lipo-chitooligosaccharide signaling in endosymbiotic plant-microbe interactions. *Mol Plant Microbe Interact* **24**: 867–878.

Huang JZ, Carney BF, Denny TP, Weissinger AK, Schell MA. (1995). A complex network regulates expression of *eps* and other virulence genes of *Pseudomonas solanacearum*. *J Bacteriol* **177**: 1259–1267.

Hubber A, Vergunst AC, Sullivan JT, Hooykaas PJJ, Ronson CW. (2004). Symbiotic phenotypes and translocated effector proteins of the *Mesorhizobium loti* strain R7A VirB/D4 type IV secretion system. *Mol Microbiol* **54**: 561–574.

Ivanov S, Fedorova E, Bisseling T. (2010). Intracellular plant microbe associations: secretory pathways and the formation of perimicrobial compartments. *Curr Opin Plant Biol* **13**: 372–377.

Limpens E, Mirabella R, Fedorova E, Franken C, Franssen H, Bisseling T *et al.* (2005). Formation of organelle-like N2-fixing symbiosomes in legume root nodules is controlled by DMI2. *Proc Natl Acad Sci USA* **102**: 10375–10380.

Madsen LH, Tirichine L, Jurkiewicz A, Sullivan JT, Heckmann AB, Bek AS *et al.* (2010). The molecular network governing nodule organogenesis and infection in the model legume *Lotus japonicus*. *Nat Commun* **1**: 10.

Marchetti M, Capela D, Glew M, Cruveiller S, Chane-Woon-Ming B, Gris C *et al.* (2010). Experimental evolution of a plant pathogen into a legume symbiont. *Plos Biol* **8**: e1000280.

Marchetti M, Catrice O, Batut J, Masson-Boivin C. (2011). *Cupriavidus taiwanensis* bacteroids in *Mimosa pudica* indeterminate nodules are not terminally differentiated. *Appl Environ Microbiol* **77**: 2161–2164.

Masson-Boivin C, Giraud E, Perret X, Batut J. (2009). Establishing nitrogen-fixing symbiosis with legumes: how many rhizobium recipes? *Trends Microbiol* **17**: 458–466.

Meng FH, Yao J, Allen C. (2011). A *motN* mutant of *Ralstonia solanacearum* is hypermotile and has reduced virulence. *J Bacteriol* **193**: 2477–2486.

Mergaert P, Uchiumi T, Alunni B, Evanno G, Cheron A, Catrice O *et al.* (2006). Eukaryotic control on bacterial cell cycle and differentiation in the Rhizobium-legume symbiosis. *Proc Natl Acad Sci USA* **103**: 5230–5235.

Momeni B, Chen C-C, Hillesland KL, Waite A, Shou W. (2011). Using artificial systems to explore the ecology and evolution of symbioses. *Cell Mol Life Sci* **68**: 1353–1368.

Moran NA. (2006). Symbiosis. *Curr Biol* **16**: R866–R871.

Ochman H, Moran N. (2001). Genes lost and genes found: evolution of bacterial pathogenesis and symbiosis. *Science* **292**: 1096–1099.

Oldroyd GED, Murray JD, S.Poole P, Downie JA. (2011). The rules of engagement in the legume-rhizobial symbiosis. *Annu Rev Genet* **45**: 119–144.

Ovchinnikova E, Journet E-P, Chabaud M, Cosson V, Ratet P, Duc G *et al.* (2011). IPD3 controls the formation of nitrogen-fixing symbiosomes in pea and *Medicago* spp. *Mol Plant Microbe Interact* **24**: 1333–1344.

Pelosi L, Kühn L, Guetta D, Garin J, Geiselmann J, Lenski RE *et al.* (2006). Parallel changes in global protein profiles during long-term experimental evolution in *Escherichia coli*. *Genetics* **173**: 1851–1869.

Plener L, Manfredi P, Valls M, Genin S. (2010). PrhG, a transcriptional regulator responding to growth conditions, is involved in the control of the type III secretion system regulon in *Ralstonia solanacearum*. *J Bacteriol* **192**: 1011–1019.

Popa O, Dagan T. (2011). Trends and barriers to lateral gene transfer in prokaryotes. *Curr Opin Microbiol* **14**: 615–623.

Poueymiro M, Genin S. (2009). Secreted proteins from *Ralstonia solanacearum*: a hundred tricks to kill a plant. *Curr Opin Microbiol* **12**: 44–52.

Ramsay JP, Sullivan JT, Jambari N, Ortori CA, Heeb S, Williams P *et al.* (2009). A LuxRI-family regulatory system controls excision and transfer of the *Mesorhizobium loti* strain R7A symbiosis island by activating expression of two conserved hypothetical genes. *Mol Microbiol* **73**: 1141–1155.

Ramsay JP, Sullivan JT, Stuart GS, Lamont IL, Ronson CW. (2006). Excision and transfer of the *Mesorhizobium loti* R7A symbiosis island requires an integrase IntS, a novel recombination directionality factor RdfS, and a putative relaxase RlxS. *Mol Microbiol* **62**: 723–734.

Rogel M, Hernández-Lucas I, Kuykendall L, Balkwill D, Martinez-Romero E. (2001). Nitrogen-fixing nodules with *Ensifer adhaerens* harboring *Rhizobium tropici* symbiotic plasmids. *Appl Environ Microbiol* **67**: 3264–3268.

Sachs JL, Skophammer RG, Regus JU. (2011). Evolutionary transitions in bacterial symbiosis. *Proc Natl Acad Sci USA* **108**: 10800–10807.

Salanoubat M, Genin S, Artiguenave F, Gouzy J, Mangenot S, Arlat M *et al.* (2002). Genome sequence of the plant pathogen *Ralstonia solanacearum*. *Nature* **415**: 497–502.

Schell MA, Denny TP, Huang JZ. (1994). VsrA, a second two-component sensor regulating virulence genes of *Pseudomonas solanacearum*. *Mol Microbiol* **11**: 489–500.

Schneider P, Jacobs JM, Neres J, Aldrich CC, Allen C, Nett M *et al.* (2009). The global virulence regulators VsrAD and PhcA control secondary metabolism in the plant pathogen *Ralstonia solanacearum*. *Chembiochem* **10**: 2730–2732.

Smillie CS, Smith MB, Friedman J, Cordero OX, David LA, Alm EJ. (2011). Ecology drives a global network of gene exchange connecting the human microbiome. *Nature* **480**: 241–244.

Sprent JI. (2001). *Nodulation in Legumes*. Royal Botanic gardens: Kew, UK.

Sprent JI. (2007). Evolving ideas of legume evolution and diversity: a taxonomic perspective on the occurrence of nodulation. *New Phytol* **174**: 11–25.

Sullivan J, Ronson C. (1998). Evolution of rhizobia by acquisition of a 500-kb symbiosis island that integrates into a phe-tRNA gene. *Proc Natl Acad Sci USA* **95**: 5145–5149.

Turner SL, Young JPW. (2000). The glutamine synthetases of rhizobia: phylogenetics and evolutionary implications. *Mol Biol Evol* **17**: 309–319.

Valls M, Genin S, Boucher C. (2006). Integrated regulation of the type III secretion system and other virulence determinants in *Ralstonia solanacearum*. *Plos Pathog* **2**: 798–807.

Yang SM, Tang F, Gao MQ, Krishnan HB, Zhu HY. (2010). R gene-controlled host specificity in the legume-rhizobia symbiosis. *Proc Natl Acad Sci USA* **107**: 18735–18740.

Supplementary Information accompanies this paper on The ISME Journal website (http://www.nature.com/ismej)